

## BOND SPLITTING STRENGTH OF CONCRETE MEMBERS REINFORCED WITH FRP BARS

Toshiyuki KANAKUBO\*, Kcisuke YONEMARU\*\*, Hiroshi FUKUYAMA\*\*\*  
and Yasuhisa SONOBE\*\*\*\*

### ABSTRACT

Two series of tests were conducted to investigate the bond splitting strength of concrete members reinforced with FRP bars. One is a simple bond test and the other is a cantilever type bond test. Bond splitting strength is discussed both for the case of no lateral reinforcement ( $\tau_{\infty}$ ) and the increment of the strength caused by lateral reinforcement ( $\tau_{st}$ ), including the results of the previous study. The result shows that both strengths are influenced by the elastic modulus of longitudinal bar. A new formula to predict the bond splitting strength for FRP bars is proposed. The result of the previous study on beams is verified using the new formula. The observed maximum strengths of the beams show a good correlation with the calculated strengths.

### 1. INTRODUCTION

Nowadays, much research concerning FRP reinforcement (FRPR) has been carried out in order to use it as a substitute for steel reinforcement in concrete construction. Although FRPR is advantageous of being lightweight, high strength, highly durable, etc., there are still critical problems to be solved in order to adopt it as a reinforcement in concrete structures. Some of which are: poor fire resistance, no plastic behavior, low stiffness, and unknown structural performance. Additional research is necessary to develop FRPR more fully for actual usage.

Bond splitting failure is caused by the splitting of concrete due to the ring tensile force around the longitudinal bars. Steel reinforced concrete members are designed so that will not occur such failure. A good bond performance is particularly essential for FRP

---

\* Graduate School, University of Tsukuba, Japan

\*\* New Construction Material Technology Division, Shimizu Corporation, Japan

\*\*\* Structural Eng. Department, Building Research Institute, Ministry of Construction, Japan

\*\*\*\* Institute of Eng. Mechanics, University of Tsukuba, Japan

reinforced concrete members to have an effective use of high tensile strength of FRPR. The authors have previously carried out a study on the bond performance of FRP reinforced concrete (1). Simple bond test, cantilever type bond test and antisymmetrical loading test were conducted. According to the results, bond performance is affected by the types of FRPR used for longitudinal bars. The bond performance in beams can be expected from the test results of cantilever type specimens with bond length of 23 times FRPR diameter. However, a general method to predict the bond splitting strength is unknown yet in the above mentioned study.

The purpose of this research is to propose a method to predict the bond splitting strength of FRPR, taking into account the results of the previous study. In this research, cantilever type specimens similar to those of the previous study (1) are mainly used. The simple type specimens (1), by which bond splitting failure can occur easily with a stress condition almost similar to that acting in members, are also utilized. The bond length of the simple type specimens is equal to that of the cantilever type specimens in this research. The test results obtained from the simple type specimens are compared with those of the cantilever type ones. Both test results are discussed for proposing a new formula to predict the bond splitting strength of FRPR. The result of the previous study on beams is also discussed in the later part using the proposed formula.

## 2. TEST PROGRAM

### 2.1 Characteristics of FRPR

The characteristics of FRPR used in this research are shown in Table 1.

Table 1 Characteristics of FRPR

Material	Identification	Nominal Diameter $D$ (mm)	Shape	Ave. Diameter $d$ (mm)	$h/d$ (%)	Tensile Strength (MPa)	Elastic Modulus (GPa)
Carbon	C128S	12 $\phi$	Braided*	12.2	7.68	1340	98.1
	C64	8 $\phi$	Braided	-	-	1340	98.1
	C32	6 $\phi$	Braided	-	-	1340	98.1
	CFRP13	13 $\phi$	Spiral	13.3	5.28	1490	120
	CFRP8	8 $\phi$	Spiral	-	-	1620	128
	CFRP6	6 $\phi$	Spiral	-	-	1620	128
Aramid	K128S	12 $\phi$	Braided*	11.5	10.3	1300	61.8
	K64	8 $\phi$	Braided	-	-	1300	61.8
	K32	6 $\phi$	Braided	-	-	1300	61.8
Glass	GFRP13	13 $\phi$	Spiral	13.5	5.72	880	43.0
	GFRP8	8 $\phi$	Spiral	-	-	732	33.7
	GFRP6	6 $\phi$	Spiral	-	-	477	27.9
Steel	D13	13 $\phi$	Deformed	12.8	4.45	1010	200
	U5.1	5.1 $\phi$	Deformed	-	-	1390	197

\* Sand coating

Three types of materials: carbon, aramid and glass, and two different shapes: braided and spiral type are used. High strength steel bars are also tested to compare with the results of FRPR. FRPR of C128S, CFRP13, K128S, GFRP13 and steel bar D13 are used as longitudinal bars. The rests of the reinforcements are used as lateral reinforcement. Sand is applied on the surface of C128S and K128S. Nominal diameter ( $D$ ) of FRPR is provided by each manufacturer. A unified definition, average diameter ( $d$ ), is used. It is obtained by measuring the maximum and minimum diameter at five points along the bar. The lug height ( $h$ ) obtained in a similar way to that in the average diameter is also used as an index which represents the grade of roughness of surface. The values of  $d$  and  $h/d$  are shown in Table 1. The elastic moduli of carbon, aramid and glass FRPR are about 100–130, 60, and 40 GPa, respectively.

## 2. 2 Specimens

The dimensions of simple type specimens are shown in Fig. 1, and the list is shown in Table 2. The size of the specimen is 600 mm in length and 240 mm in depth. The bond length is 300 mm, that is about 23 times the diameter of FRPR. An unbonded region is set at the right half portion of the specimen. A steel plate and rubber are placed at the center of the specimen to allow lateral deformation of the bonded concrete. One longitudinal bar is placed at the center of the cross section to get the bond splitting called side split mode (1). Normal weight concrete was cast in the direction shown in Fig. 1. The bar is set as the bottom side longitudinal bar of a beam. Three specimens were tested for one type of FRPR.

The cantilever type specimens are listed in Table 3, and their dimensions are shown in Fig. 2. The specimens are 200 mm in width ( $b$ ) and 350 mm in depth, with a bond length similar to the simple type specimens of 300 mm. Unbonded regions are set at the loaded and free ends of the specimen. The test variables are: types of longitudinal bars and lateral reinforcement, and percentage of lateral reinforcement ( $p_w$ ). Normal weight concrete was cast horizontally from the top side.

**Table 2** List of simple type specimens

No.	Longitudinal Bar	Note
1~3	CFRP13	Concrete compressive strength = 34.3 MPa
4~6	GFRP13	
7~9	C128S	
10~12	K128S	
13~15	D13	

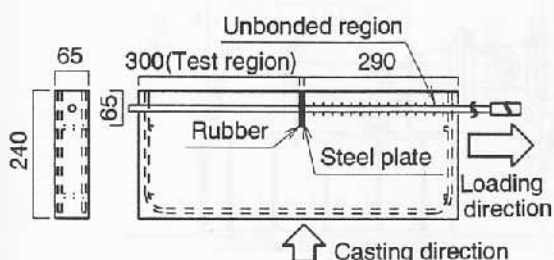


**Fig. 1** Simple type specimen

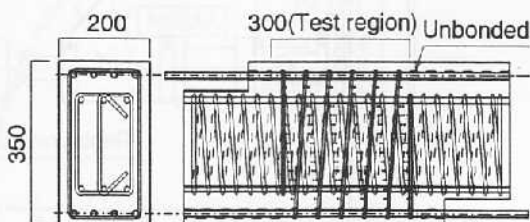


**Fig. 2** Cantilever type specimen

**Table 3** List of cantilever type specimens

No.	Identifi- cation	Longitudi- nal Bars	Lateral	Reinf.	No.	Identifi- cation	Longitudi- nal Bars	Lateral	Reinf.
			Arrangement	$p_w$ (%)				Arrangement	$p_w$ (%)
1	N36T-	CFRP13	-	0.00	13	N36A-	K128S	-	0.00
2	N36TT40		CFRP6@70	0.40	14	N36AA40		K32@63	0.40
3	N36TT80		CFRP6@35	0.81	15	N36AA80		K32@31	0.81
4	N36TT120		CFRP8@42	1.20	16	N36AA120		K64@42	1.19
5	N36G-	GFRP13	-	0.00	17	N36CA80	C128S	K32@31	0.81
6	N36GG40		GFRP6@70	0.40	18	N36CS80		U5.1@26	0.78
7	N36GG80		GFRP6@35	0.81	19	N36AC80	K128S	C32@31	0.81
8	N36GG120		GFRP8@42	1.20	20	N36AS80		U5.1@26	0.78
9	N36C-	C128S	-	0.00	21	N36SC80	D13	C32@31	0.81
10	N36CC40		C32@63	0.40	22	N36SA80		K32@31	0.81
11	N36CC80		C32@31	0.81	23	N36SS80		U5.1@26	0.78
12	N36CC120		C64@42	1.19					

Identification: N36 C A 80  
a b c d

a: concrete;

b: longitudinal bar;

c: lateral reinforcement;

d: lateral reinf. ratio ( $p_w$ ); 40 = 0.4%, 80 = 0.8%, 120 = 1.2%

N36 = normal weight concrete with specified compressive strength of 35MPa

T = CFRP, G = GFRP, C = C128S, A = K128S, S = D13

T = CFRP, G = GFRP, C = C32 or C64, A = K32 or K64, S = U5.1,  
- = no lateral reinforcement

Measured compressive strength of concrete:

No.1 ~ 14 = 33.1 MPa, No.17, 18, 21, 22, 23 = 33.9 MPa, No.15, 16, 19, 20 = 34.3 MPa

## 2.3 Loading and Measurement

In the cantilever type bond test and in the simple bond test, longitudinal bars were pulled out monotonically. The loading system used in the cantilever type bond test is shown in Fig. 3. In this test, once the top bars were pulled out, the specimens were turned over and the loading of the bottom bars was done in the same way. In both tests, pull out load and slips of longitudinal bars at the loaded and free ends were measured. In the cantilever type bond test, strains of reinforcements were measured at some points.

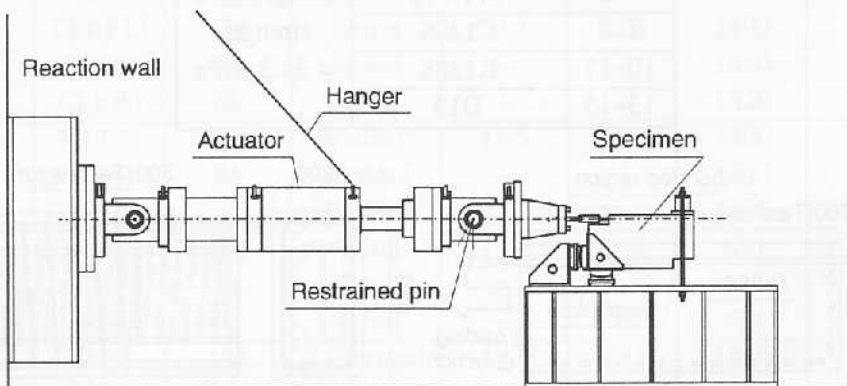


**Fig. 3** Loading system of cantilever type bond test

### 3. TEST RESULTS

#### 3. 1 Simple Bond Test

All specimens failed by bond splitting called side split mode. The observed bond splitting strengths ( $\tau_{co}$ ) are shown in Fig. 4. Differences on the strength can be observed. This is due to the types of longitudinal bars. The strengths are almost the same among three specimens with the same bars.

#### 3. 2 Cantilever Type Bond Test

Failure in all specimens is caused by bond splitting called side split mode. Fig. 5 shows some examples of the bond stress ( $\tau$ ) versus loaded end slip curves. As the percentage of lateral reinforcement ( $p_w$ ) increases, an increment of the maximum bond stress and gradual decrement after the maximum stress can be observed. However, there is a negligible difference in the maximum stress between the specimens with  $p_w = 1.2\%$  and those with  $p_w = 0.8\%$  among some types of FRPR.

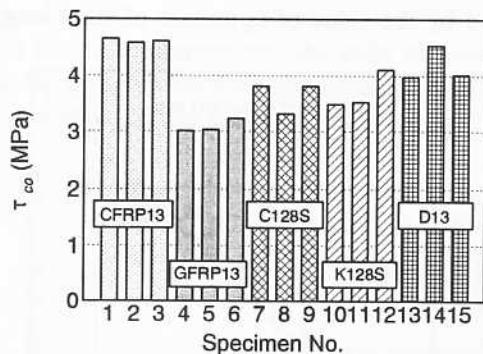


Fig. 4 Bond splitting strength of simple type specimen

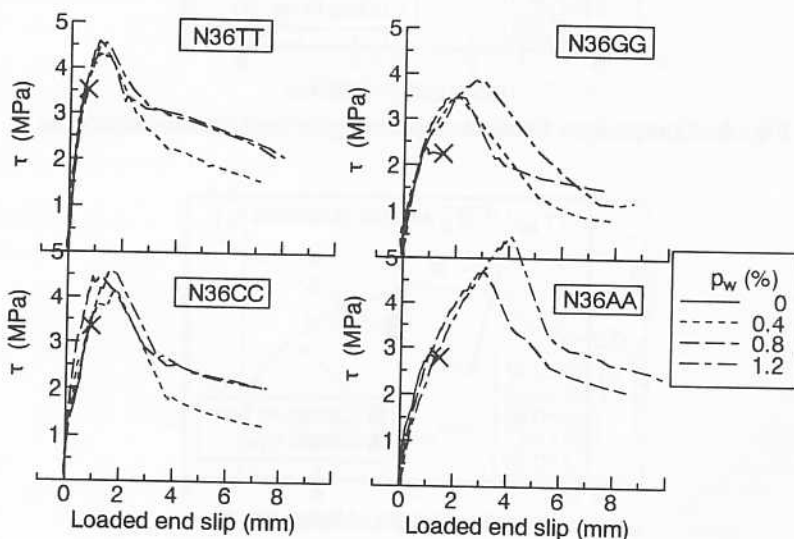


Fig. 5 Bond stress - loaded end slip curves of cantilever type specimens

A comparison between bond splitting strengths ( $\epsilon\tau_{bu}$ ) obtained for top bars and those for bottom bars in this and the previous study (1) is shown in Fig. 6. In this research, the bond splitting strength ratio of top bars to bottom bars is 1.00, whereas the ratio obtained for all the data including those in the previous study is 0.97. Discussions on the bottom strength will be presented later. The top strength is made comparable to the bottom strength.

#### 4. BOND SPLITTING STRENGTH OF FRPR

##### 4. 1 Discussion on the Strength of Simple Type Specimen

A formula to predict the bond splitting strength in the case of no lateral reinforcement was proposed for ordinary steel reinforced concrete members as shown in Fig. 7 ( $\epsilon\tau_{bu}$ ) (2). Fig. 7 shows the correlation between the normalized length of failure line ( $b_i$ ) (2) and the observed strength ( $\epsilon\tau_{bu}$ ) normalized by the square root of concrete compressive strength ( $\sigma_B$ ). The data are obtained from the specimens having steel longitudinal bars (D13) without lateral reinforcement. The straight line shows the calculated value using the formula. The points are located near the line. Therefore, the bond splitting strength obtained for the simple type specimens is also confirmed by the value of  $b_i$  in case of steel longitudinal bar.

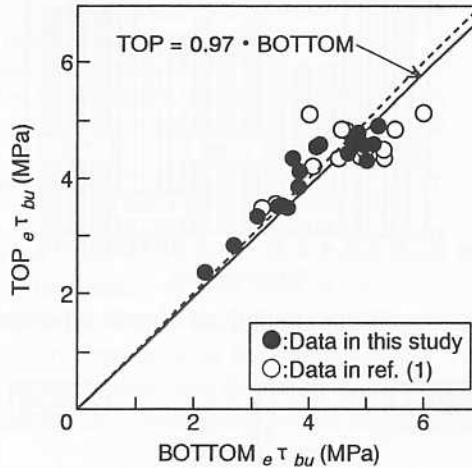


Fig. 6 Comparison between top strengths and bottom strengths

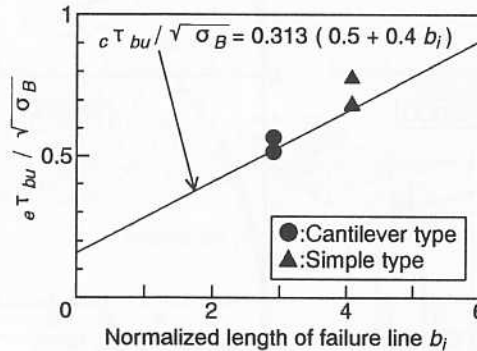


Fig. 7 Strength of steel longitudinal bars

Fig. 8 shows the correlation of the observed bond splitting strength ( $\tau_{bu}$ ) between the simple type specimens and the cantilever type specimens without lateral reinforcement in the same type of FRPR. The observed strengths are normalized by the calculated value ( $c\tau_{bu}$ ) explained in the preceding paragraph. X versus Y relationship shows one to one correspondence in spite of different types of FRPR. Therefore, the bond splitting strength of the cantilever type specimen can be evaluated using the result obtained for the simple type specimen without lateral reinforcement.

#### 4. 2 Bond Splitting Strength without Lateral Reinforcement

It is considered that the bond splitting strength is influenced by the elastic modulus, shape, and surface treatment of FRPR. The value of  $h/d$  (section 2. 1) is one of the indexes which express how shape and surface treatment influence the strength. As shown in Fig. 4, the bond splitting strengths of CFRP13 are different from those of GFRP13. However, both FRPRs have almost the same value of  $h/d$  (Table 1). It can not be recognized that the strength increases as the value of  $h/d$  also increases. Therefore, it is considered that the surface shape of FRPR does not influence the bond splitting strength. However, it is necessary that bond splitting failure of concrete will be caused by the FRPR.

In the case of no lateral reinforcement, the ratio of obtained strength to calculated value using the formula for ordinary steel reinforced concrete (2) is defined as a reduction factor,  $K_{co}$ . This is used in evaluating the influence of elastic modulus of FRPR. Fig. 9 shows

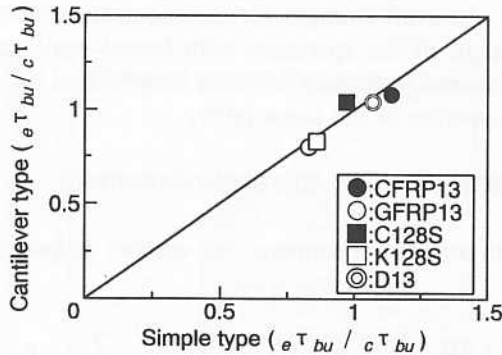


Fig. 8 Strength of cantilever and simple type specimens

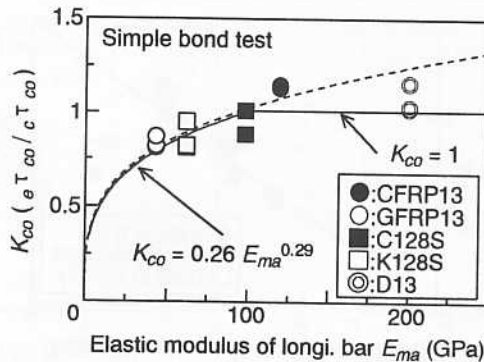


Fig. 9 Correlation between  $E_{ma}$  and  $K_{co}$

the correlation between the elastic modulus of longitudinal bar,  $E_{ma}$  (unit: GPa), and  $K_{co}$ . This is obtained using the data of the simple type specimens. As the value of  $E_{ma}$  decreases,  $K_{co}$  also decreases. The correlation among the data of FRPR is calculated by the regression analysis wherein formula (1) is obtained. The value of  $K_{co}$  should be 1 when  $K_{co}$  exceeds 1.

$$\begin{cases} K_{co} = 0.26 E_{ma}^{0.29} & (E_{ma} < 102) \\ K_{co} = 1 & (E_{ma} \geq 102) \end{cases} \quad (1)$$

where,  $K_{co}$  : reduction factor for bond splitting strength without lateral reinforcement  
 $E_{ma}$  : elastic modulus of longitudinal bar (GPa)

The bond splitting strength of FRPR without lateral reinforcement is presented as follows:

$$\tau_{co} = 0.313 (0.5 + 0.4 b_i) \sqrt{\sigma_B} \cdot K_{co} \quad (2)$$

(Notations can be referred to in the appendix.)

The correlation between the observed strength and the calculated value using formula (2) in the present and the previous study (1) is shown in Fig. 10. A good relationship between the observed and the calculated values can be observed.

#### 4. 3 Increment of Bond Splitting Strength Caused by Lateral Reinforcement

The increment of bond splitting strength caused by lateral reinforcement ( $\tau_{st}$ ) is calculated by subtracting observed strength for the specimen without lateral reinforcement ( $\tau_{co}$ ) from observed strength of the specimen with lateral reinforcement ( $\tau_{bu}$ ). Using the measured strain,  $\tau_{bu}$  is obtained separately for each longitudinal bar, located at the corner or at the center of the cross section in the same layer.

##### (1) Steel longitudinal bars with FRP lateral reinforcement

For normal weight concrete specimens, the authors proposed the following formula to predict  $\tau_{st}$  (1):

$$\tau_{st} / \sqrt{\sigma_B} = 0.313 (10 N_c / N_t + 5 N_u / N_t) \cdot (b / d_b) \cdot p_w \cdot (E_{st} / E_s)^{0.21} \quad (3)$$

where,  $E_{st}$  : elastic modulus of lateral reinforcement

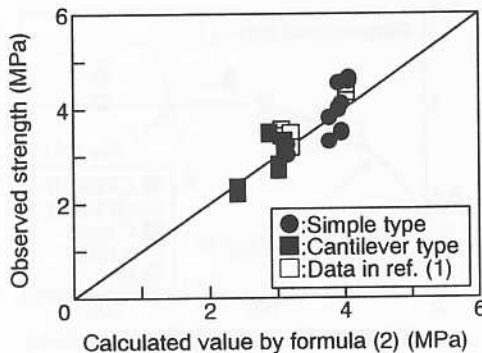


Fig. 10 Comparison of observed strength and calculated value

$E_s$  : elastic modulus of steel

Other notations can be referred to in the appendix.

Fig. 11 shows the correlation between the observed strength and the calculated value using formula (3) in the present and the previous data (1). In case of steel longitudinal bars, the bond splitting strength can be evaluated using formula (3).

## (2) FRP longitudinal bars with FRP lateral reinforcement

The difference in the strength between corner and center bars is observed in steel longitudinal bars (1). Fig. 12 shows the comparison between the observed strength ( $e\tau_{st}$ ) at the corner and at the center in specimens with FRP longitudinal bars. The straight line shows the ratio of the strength of corner bar to that of center bar of 1 : 1. The strength ratio of corner bars to center bars is 1.05 on the average. There is almost no difference in the strength because the values of  $e\tau_{st}$  are relatively smaller than the values of  $\tau_{co}$ . Besides, the data are scattered. The strength of center bar is assumed to be equal to that of corner bar in the following discussions.

The correlation between the elastic modulus of lateral reinforcement ( $E_{st}$ ) and  $e\tau_{st}$  is shown in Fig. 13. This is for specimens with  $p_w = 0.8\%$ . The strength is slightly influenced by the difference of  $E_{st}$ . The authors have proven that the  $\tau_{st}$  is influenced not only by the types of lateral reinforcement but also by the types of longitudinal bars (1). This little difference of the strength supports this conclusion.

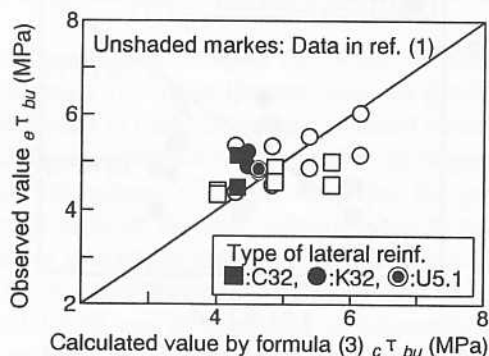


Fig. 11 Strength of steel longitudinal bars with FRP lateral reinforcement

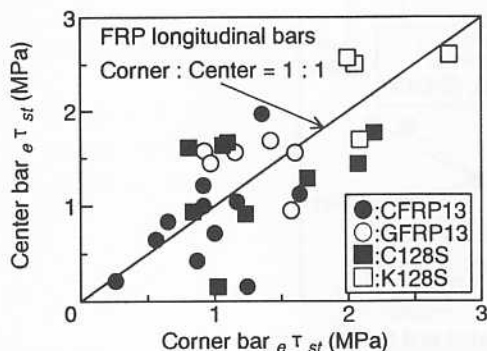


Fig. 12 Comparison of center to corner bar

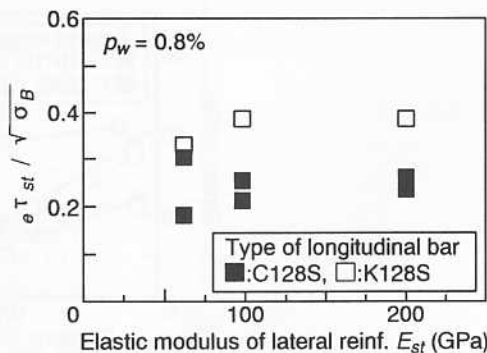


Fig. 13 Correlation between  $E_{st}$  and  $e\tau_{st}$

The correlation between the ratio of lateral reinforcement to the diameter of longitudinal bar ( $b/d_b \cdot p_w$ ) and  $\epsilon \tau_{st}$  for each type of longitudinal bar is shown in Fig. 14. The straight lines show the results of the regression analysis for each type of longitudinal bar. With the slopes denoted as  $K_{st}$ , the following formula is obtained for each type of longitudinal bar:

$$\tau_{st} = K_{st} \cdot (b / d_b) \cdot p_w \sqrt{\sigma_B} \quad (4)$$

where,  $K_{st}$  : constant which expresses the rate of increment of bond splitting strength caused by lateral reinforcement

Other notations can be referred to in the appendix.

It is considered that the elastic modulus of longitudinal bar has an influence on the transmission of bond stress. The effective length transferring the bond stress seems to change by the types of longitudinal bars (1). It can be assumed that a similar phenomenon occurs on the confinement effect of longitudinal bars for bond splitting caused by lateral reinforcement. Fig. 15 shows the stress distributions of lateral reinforcements for specimens with  $p_w = 0.8\%$ . The data are obtained by measuring strains when the pull out load reaches the maximum value. The great bond stress is observed locally for the longitudinal bars with lower elastic moduli (GFRP13, K128S). The stress distributions have a similar tendency among the bars with almost the same elastic moduli.

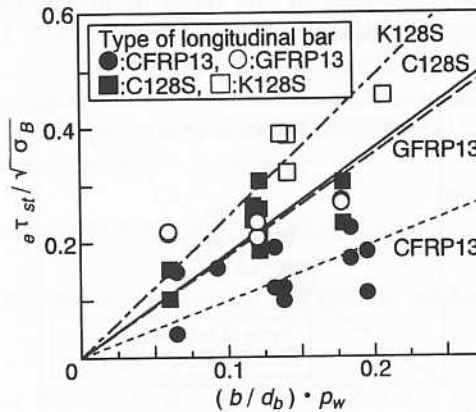


Fig. 14 Correlation between  $(b/d_b) \cdot p_w$  and  $\epsilon \tau_{st}$

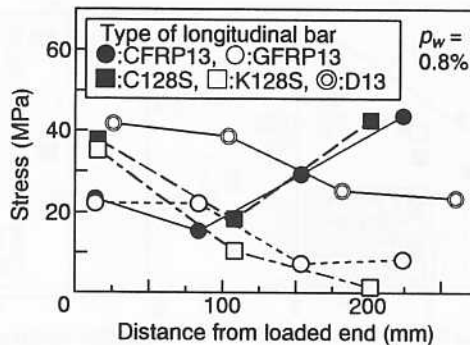


Fig. 15 Stress distribution of lateral reinforcement at the maximum load

The correlation between the elastic modulus of longitudinal bar ( $E_{ma}$ ) and  $K_{st}$  is shown in Fig. 16. The value of  $K_{st}$  generally increases as the value of  $E_{ma}$  decreases. The following formula is obtained by the regression analysis:

$$K_{st} = 15.8 E_{ma}^{-0.52} \quad (5)$$

(Notations can be referred to in the appendix.)

#### 4. 4 Verification of Obtained Formula

The bond splitting strength of FRP reinforced concrete members can be evaluated by the following formula. The applicable range for elastic modulus of longitudinal bar is also defined as follows, taking into account the types of studied FRPR:

$$\tau_{bu} = \{ (0.4 b_i + 0.5) K_{co} + K_{st} (b / d_b) p_w \} \sqrt{\sigma_B} \quad (6)$$

where,  $K_{co}$  : reduction factor for bond splitting strength without lateral reinforcement;

$$\begin{cases} K_{co} = 0.26 E_{ma}^{0.29} & (E_{ma} < 102) \\ K_{co} = 1 & (E_{ma} \geq 102) \end{cases}$$

$K_{st}$  : constant which expresses the rate of increment of bond splitting strength caused by lateral reinforcement;

$$K_{st} = 15.8 E_{ma}^{-0.52}$$

$E_{ma}$  : elastic modulus of longitudinal bar (GPa) provided that;  
 $43.0 \leq E_{ma} \leq 120$

Other notations can be referred to in the appendix.

Fig. 17 shows the correlation between the observed bond splitting strength and the calculated value using formula (6) in the present and the previous study (1). The data of lightweight concrete specimens (1) are shown as unshaded circles. The calculated values of specimens with  $p_w > 1.2\%$  are assumed to be equal to those with  $p_w = 1.2\%$ , because the maximum strength dose not exceed a certain value for the greater lateral reinforcement (section 3. 2). The average ratio of the observed strengths to the calculated values is 1.06, and their standard deviation is 0.10 for normal weight concrete specimens. The average and standard deviation for lightweight concrete specimens is 0.78 and 0.10, respectively. The bond splitting strength of FRPR can be evaluated satisfactorily using formula (6).

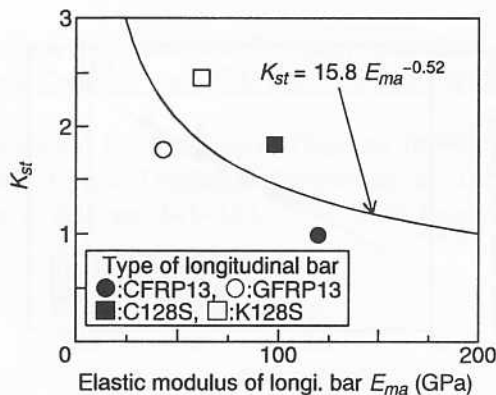
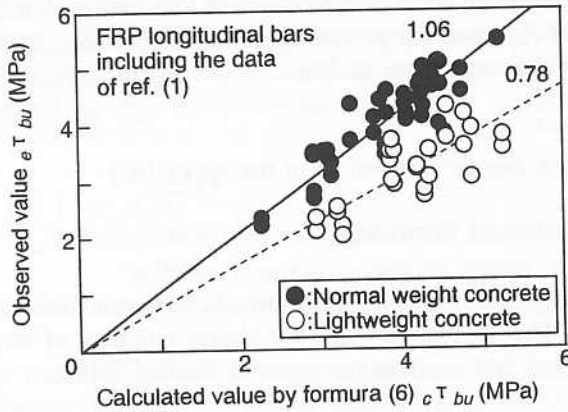


Fig. 16 Correlation between  $E_{ma}$  and  $K_{st}$



**Fig. 17** Comparison between observed strength and calculated value (cantilever type specimens)

The obtained data for 8 beams in the previous studies (1,3) are verified using formula (6) in the following discussion. Six beams have CFRP longitudinal bars with CFRP lateral reinforcement. The other two beams have steel longitudinal bars with CFRP or aramid lateral reinforcement. All beams failed by bond splitting. Fig. 18 shows the correlation between bond capacity ( $c\tau_{bu} / c\tau_{ave.}$ ) (1) and observed maximum loads ( $eQ_{max}$ ). The maximum load is normalized by the bending strength ( $eQ_{mu}$ ) calculated by fiber analysis (1).  $c\tau_{bu}$  is calculated using formula (6) with  $p_w \leq 1.2\%$ . The data are located almost on a line similar to that obtained in Reference (1). This leads to the following formula obtained by the least square method:

$$eQ_{max} / eQ_{mu} = 0.53 c\tau_{bu} / c\tau_{ave.} + 0.22 \quad (7)$$

where,

- $eQ_{max}$  : observed maximum load
- $eQ_{mu}$  : calculated bending strength
- $c\tau_{bu} / c\tau_{ave.}$  : bond capacity
- $c\tau_{bu}$  : calculated bond splitting strength
- $c\tau_{ave.}$  : average bond stress for longitudinal bar of beam

The maximum load of a beam, which fails by bond splitting, can be evaluated using formula (7). When the value of  $eQ_{max} / eQ_{mu}$  is 1, the value of bond capacity becomes 1.48.

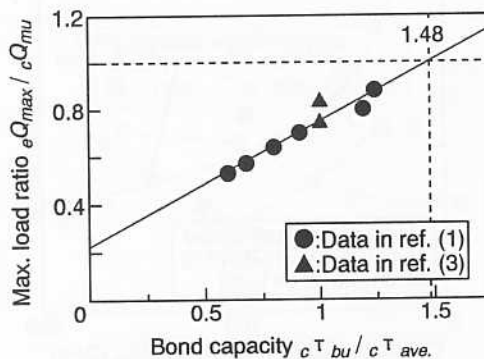


**Fig. 18** Correlation between bond capacity and the maximum load

This means that a member with bond capacity equal to or less than 1.48 will fail by bond splitting. However, it is supposed that for a member with a bond capacity smaller than 1, it will fail by bond splitting. It is considered that the difference of 0.48 ( $1.48 - 1$ ) is due to the influence of cyclic loading on the beams.

## 5. CONCLUSION

- 1) In the case of no lateral reinforcement, bond splitting strength of the cantilever type specimen can be evaluated using the result obtained for the simple type specimen.
- 2) Bond splitting strength without lateral reinforcement ( $\tau_{co}$ ) can be evaluated using the reduction factor ( $K_{co}$ ), which is a function of elastic modulus of longitudinal bar ( $E_{ma}$ ).
- 3) The difference in the bond splitting strength between corner and center bars can not be observed in specimens with FRP longitudinal bars. The increment of bond splitting strength ( $\tau_{st}$ ) is also given as a function of elastic modulus of longitudinal bar.
- 4) The maximum load of a beam, which fails by bond splitting, can be evaluated by the value of bond capacity which is calculated using the obtained formula.

## ACKNOWLEDGEMENT

This research is conducted under the National Research Project on the Use of New Materials in Construction Field sponsored by the Ministry of Construction of Japan. The authors wish to express gratitude to the members of the project and to Mr. M. Fujisawa of Tsukuba College of Technology for his kind support.

## REFERENCES

- (1) Kanakubo T., et al, "Bond Performance of Concrete Members Reinforced with FRP Bars," Fiber-Reinforced-Plastic Reinforcement for Concrete Structures -International Symposium-, ACI, SP-138, pp. 767~788, 1993
- (2) AIJ, "Design Guidelines for Earthquake Resistant Reinforced Concrete Buildings Based on Ultimate Strength Concept," pp. 135~141, 1990 (in Japanese)
- (3) Sonobe Y., et al, "Flexural Performance of Concrete Beams Reinforced with FRP Bars under Antisymmetric Cyclic Loading," Summaries of Technical Papers of Annual Meeting, Structures 2, AIJ, pp. 141~144, 1992. 8 (in Japanese)

## APPENDIX

### Notations

$a_w$  : sectional area of a pair of lateral reinforcements

- $b$  : width of member  
 $b_i$  : normalized length of failure line ( $= (b - N_t \cdot d_b) / N_t$ )  
 $d$  : average diameter of reinforcement  
 $d_b$  : diameter of longitudinal bar  
 $E_{ma}$  : elastic modulus of longitudinal bar (GPa)  
 $E_s$  : elastic modulus of steel ( $= 206$  GPa)  
 $E_{st}$  : elastic modulus of lateral reinforcement (GPa)  
 $h$  : lug height of reinforcement  
 $K_{co}$  : reduction factor for bond splitting strength without lateral reinforcement  
 $K_{st}$  : constant which expresses the rate of increment of bond splitting strength caused by lateral reinforcement  
 $N_c$  : number of corner longitudinal bars ( $= 2$ )  
 $N_t$  : number of longitudinal bars  
 $N_u$  : number of center longitudinal bars ( $= N_t - N_c$ )  
 $p_w$  : lateral reinforcement ratio ( $= a_w / b \cdot s$ )  
 $Q_{max}$  : maximum load of beam  
 $Q_{mu}$  : bending strength  
 $s$  : spacing of lateral reinforcement  
 $\sigma_B$  : compressive strength of concrete  
 $\tau$  : bond stress  
 $\tau_{ave}$  : average bond stress for longitudinal bar  
 $\tau_{bu}$  : bond splitting strength ( $= \tau_{co} + \tau_{st}$ )  
 $\tau_{co}$  : bond splitting strength without lateral reinforcement  
 $\tau_{st}$  : increment of bond splitting strength caused by lateral reinforcement

\* Subscript  $e$  before notations shows observed value and subscript  $c$  shows calculated value.